CHAPTER 9

The Bacterial Mechanosensitive Channel MscS: Emerging Principles of Gating and Modulation

Sergei Sukharev, Bradley Akitake, and Andriy Anishkin
Department of Biology, University of Maryland, College Park, Maryland 20742

Current Topics in Membranes, Volume 58
1063-5823/07 $35.00

DOI: 10.1016/S1063-5823(06)58009-3

I. OVERVIEW

The mechanosensitive channel of small conductance (MscS) is a tension-driven osmolyte release valve, which plays a critical role in bacterial adaptation to low osmolarity. Homologues of MscS have been identified in yeast and higher plants with at least two molecular species being involved in the regulation of chloroplast volume and fission. In bacteria, MscS and MscL channels are the major components of a turgor-driven emergency osmolyte efflux system. Of the two, MscS is considerably more complex, as it shows time-dependent patterns of gating and adaptation. This chapter will attempt to present a current interpretation of the main functional traits of MscS in light of its crystal structure. Responding directly to membrane tension, MscS generates either sustained or transient permeability responses cycling through at least three functional states. The response amplitude (P_o) depends on the rate of tension application, whereas the duration, defined by inactivation kinetics, depends on the magnitude of the mechanical stimulus, voltage, and presence of specific solutes. Molecular dynamics (MD) simulations data from several groups show that the pore of MscS, in the crystal conformation, is largely dehydrated and likely nonconductive. In addition, instability of the splayed crystal conformation in the lipid bilayer during simulations suggests that the crystal structure may not represent a native state for the protein. Models of the opening process, based on experimental data, depict a substantial expansion of the hydrophobic pore accompanied by a critical wetting event required for the onset of conduction. Simulations also suggest that the characteristic kink, breaking the pore-lining TM3 helix at G113, may straighten in the open conformation. Several hypotheses will be presented, based on the phenomenology and results of computational analysis, about the character of conformational transitions in MscS between its resting, open, and inactivated states, the significance of pore dehydration and the putative function of the cage-like cytoplasmic domain as an internal, solute-specific osmosensor.

II. INTRODUCTION

Osmoregulation is fundamental problem for all organisms because even relatively small osmotic imbalances can produce large and damaging volume or intracellular solute concentration changes. It is for this reason that physicians often scrutinize a patient's fluid and electrolyte balance for diagnostic clues. Although the cell physiology of osmoregulation has been studied for decades, the existing molecular information is fragmental. Even in bacteria, which are the smallest and therefore "simplest" of all free-living

organisms, the primary mechanisms of osmosensing and osmoregulation are not fully understood. Solving this puzzle of how a cell senses water activity inside and outside and then triggers multiple adaptive pathways to counteract perturbation would provide an important link between the fundamental thermodynamics of macromolecular (or membrane) solvation and organismal physiology (Wood, 1999). The study of these systems in bacteria is important for several reasons. First, understanding the mechanisms of osmosensing and the accumulation/release or exchange of compatible osmolytes in bacteria would provide insight into both the physical and evolutionary biochemistry of these systems. Second, osmoregulatory mechanisms play key roles in parasite–host or symbiont–host interactions (Stewart *et al*., 2005) and determine the environmental stability of pathogens/symbionts inside and outside of the host. Study of these mechanisms will potentially aid in fight to stop the spread of infectious diseases. It is, therefore, fortunate that these bacterial systems provide extremely convenient tools to gain a basic understanding of macromolecular function in particular for the biophysical studies of membrane proteins.

The MscS is a bacterial osmolyte release valve that limits turgor pressure during osmotic downshock, thus rescuing cells from lysis (Levina *et al*., 1999). Together with three other mechanosensitive channels, MscK (K^+ dependent), MscL (large conductance), and the yet unidentified mini-channel MscM, MscS constitutes a partially redundant system, which provides graded permeability response to osmotic stress (Berrier *et al*., 1996; Blount *et al*., 1999; Martinac, 2001; Booth *et al*., 2003). Like the large conductance channel MscL, MscS gates directly by tension developed in the surrounding lipid bilayer. In contrast to MscL, which is characterized by steady, tension-dependent, activities observed near the membrane's lytic limit (~8–12 dyne/cm), MscS responds to moderate tensions (4–6 dyne/cm) usually with a transient (decaying) response implying activation followed by transition to an inactivated or desensitized state(s) (Koprowski and Kubalski, 1998; Levina *et al*., 1999; Akitake *et al*., 2005). The crystal structures of MscL (homologue from *Mycobacterium tuberculosis*) and *Escherichia coli* MscS have been solved by Rees and coworkers (Chang *et al*., 1998; Bass *et al*., 2002) and provide critical information and a strong impetus to the field. The more elaborate structure of MscS currently guides efforts of several experimental and computational groups toward unraveling the molecular mechanism of its gating and intricate adaptive behaviors. While MscL is primarily a prokaryotic molecule, with several distant homologues in fungi, MscS-type channels appear to be more widespread (Pivetti *et al*., 2003). Multiple homologues have recently been identified in higher plants. Three such homologues in *Arabidopsis thaliana* were found to regulate the volume and division of chloroplasts (Haswell and Meyerowitz, 2006). This chapter

will provide an update focused primarily on the functional studies of *E. coli* MscS and discuss the emerging paradigms of MscS-gating mechanism in the frameworks of structural information and known principles of bacterial osmoregulation.

III. MscS AND ITS RELATIVES

A. A Brief Account of Bacterial Osmoregulation and the Discovery of MscS

Bacteria and other walled cells maintain their volumes and shape by creating positive turgor pressure in the cytoplasm against the confines of their cell wall. This is achieved through an osmotic network of solute uptake systems accompanied by *de novo* synthesis of substances that maintain normal osmotic pressure gradients across the cytoplasmic membrane. It is generally accepted that an intracellular pressure of ~3–4 atm is required for normal proliferation of enteric bacteria such as *E. coli* and much higher pressures (15–25 atm) are typical for Gram-positive species (Csonka, 1989; Wood, 1999). Under steady growth conditions, turgor pressure is collectively created by small molecular constituents such as free amino acids, polyols, nucleotides, and two major intracellular ions, K^+ and glutamate. If the medium suddenly becomes hypertonic due to increased salinity, bacterial cells initially loose turgor but quickly regain it by accumulating extra K^+ and glutamate (Epstein, 2003) through independent transport systems (McLaggan *et al.*, 1994). K^+, however, is not the most optimal intracellular osmolyte as its elevation changes the ionic strength inside the cell. Thus, having restored normal turgor, the cells gradually exchange K^+ for more inert substances such as proline, betaine, and to some extent trehalose (Csonka and Hanson, 1991). These solutes are called "compatible" as they minimally affect cellular functions, though still aid in the retention of water.

The growth conditions for enteric and soil bacteria are not always steady and periods of proliferation in high-osmolarity environments are often interrupted by low-osmolarity conditions (rain/drainage water). In these instances, previously accumulated solutes put the bacterium at risk for osmotic lysis as the peptidoglycan cell wall can restrain the volume change but only to a certain extent. It has been shown that peptidoglycan is distensible, and cell swelling results in substantial increases of internal volume (Koch and Woeste, 1992). As the excess slack of the inner membrane is used up, tension in the bilayer starts to build. Amelioration of this tension was found to occur through a drastic permeability increase of the cell membrane followed by the release small solutes to reduce the osmotic gradient (Britten and McClure, 1962; Tsapis and Kepes, 1977). This reversible permeability change, demonstrated

to take 1–2 s with little effect on cell survival, was initially interpreted as transient membrane "crack" formation or some sort of reversible membrane breakdown. Later studies (Schleyer *et al.*, 1993) refined the repertoire of released osmolytes and linked the reversible permeability pathways to the activities of bacterial stretch-activated channels first reported by the Kung laboratory (Martinac *et al.*, 1987).

By applying the standard patch-clamp technique (Hamill *et al.*, 1981) to giant spheroplast preparations (Ruthe and Adler, 1985), Martinac *et al.* (1987) first documented the presence of 1-nS pressure-activated channels in the *E. coli* cell envelope. This channel was more active under depolarizing voltages (cytoplasm positive). Its activity was also found to be dependent on the presence of K^+ as the channel was completely inactive in Na^+ buffers. Further studies involving membrane solubilization and reconstitution experiments (Sukharev *et al.*, 1993) revealed that *E. coli* possesses two distinct mechanically activated channel species, one of smaller (1 nS) conductance, similar to those previously observed by Martinac and designated as MscS, and a channel with three times larger (3.2 nS) conductance and spiky activities named MscL. The MscL protein was subsequently isolated and its gene cloned (Sukharev *et al.*, 1994). Surprisingly, it was found that the *mscL*-null mutant did not exhibit any growth/survival phenotype under a variety of osmotic conditions.

Identification and cloning of MscS and MscK by the Booth laboratory came in 1999 through studies of mutations which altered K^+ exchange with betaine and genomic analysis of related sequences (Levina *et al.*, 1999). In the event of osmotic upshock, primary K^+ uptake is mediated by the Trk, Ktr, and Kdp pumps activated by low turgor (Epstein, 2003). The subsequent accumulation of proline and betaine is accomplished by the ProU, ProP, and BetT active transporters, which also fulfill the roles of osmosensors (Wood *et al.*, 2001). While searching for the K^+ efflux and accompanying proline–betaine uptake pathways, Booth and collaborators studied the *kefA*, *kefB*, and *kefC* loci. The two latter systems were found to be active primarily under toxic or oxidative stresses (Ferguson *et al.*, 2000). A *kefA*-null mutation did not change the course of betaine-for-K^+ exchange under high osmolarity either, but a point mutation in *kefA* (called RQ2) exhibited a growth-suppressing phenotype when the cells were grown in a high-osmotic medium in the presence of K^+ and betaine. The RQ2 bacteria accumulated betaine normally, but were unable to extrude K^+ efficiently and became extremely sensitive to turgor created by the two osmolytes (McLaggan *et al.*, 2002). From this phenotype, it seemed possible that the product of *kefA* was a stretch-sensitive membrane protein. The *kefA* open reading frame coded for a large (1120 amino acid) multidomain membrane protein. The search for *E. coli* sequences similar to *kefA* revealed two proteins of the same length

(AefA and YjeP) and a smaller protein resembling the C-terminal part of KefA, named YggB. Generation of single and multiple null mutants followed by reexpression of individual genes "in *trans*" revealed that *kefA* and *yggB* both code for mechanosensitive channels of similar 1-nS conductance. KefA, characterized by sustained activities under constant pressure gradients, was shown to be dependent on the presence of K^+ (Levina *et al.*, 1999), thus it was renamed MscK. The product of *yggB*, which was more abundant and generated transient responses to pressure steps, was renamed MscS. None of the other related open reading frames (ORFs) produced measurable channel activities *in situ*. It was discovered that the generated triple *mscK*-, *mscS*-, *mscL*-knockout strain (MJF465) had increased sensitivity to moderate downshocks (400–500 mOsm), and reexpression of either MscL or MscS fully restored the osmotic downshift tolerance to wild-type (WT) levels. Expression of MscK alone in the triple knockout strain did not ameliorate its osmotic fragility (Levina *et al.*, 1999). This ground-breaking work not only identified two new genes for mechanosensitive channels of very similar conductance (previously though to be one), but also unequivocally demonstrated the partially redundant physiological roles for MscS and MscL as turgor-limiting release valves. In addition, MJF 465 has become a highly useful "clean" background system for mechanosensitive channel expression, electrophysiology recording, and testing of the osmotically driven rescuing ability of multiple MscS and MscL mutants.

B. MscS Vs MscK: How to Interpret Early Functional Data?

The earliest functional studies of *MscS-like* mechanosensitive channels in *E. coli* spheroplasts conducted by Martinac *et al.* reported on a population of pressure-sensitive ion channels of ~1-nS conductance. Single channel recordings revealed pressure dependence, a strong and sharp increase of channel open probability observed with increasing suction, and voltage dependence. Increasingly depolarizing voltages made the channel population easier to open and shifted the activation curves progressively to the left. Subsequent study of these channels in the whole-protoplast recording mode by Cui *et al.* (1995) revealed similar phenomenology.

Data from these early studies were obviously collected on mixed populations of channels, and it is now known that a WT *E. coli* background contains both MscS and MscK with similar activities. Of the two, MscK is a much larger multidomain protein. From an alignment of the primary sequences, the 286- amino acid-long MscS shares 23% identity and 53% similarity to the C-terminal part of MscK. Although these numbers are not quite high enough to conclude structural identity, analysis of the residue

patterns, especially those in the transmembrane (TM) region, suggested very similar organization, and provides some rationale for their similar gating characteristics (Levina *et al.*, 1999; Miller *et al.*, 2003a). PhoA-fusion experiments concluded that the common parts of MscK and MscS each contain three TM domains, with the N-terminal ends of the protein being periplasmic and the larger soluble C-terminal domains residing in the cytoplasm (Miller *et al.*, 2003a). MscK also has a large N-terminal domain that was predicted to form up to seven additional TM spans. In spite of the structural differences, both channels were characterized with similar ~1-nS conductances, a slight anionic preference, and weak inward rectification (Li *et al.*, 2002).

Studies of MscS expressed in a clean genetic background (Levina *et al.*, 1999; Vasquez and Perozo, 2004; Akitake *et al.*, 2005) revealed functional characteristics that substantially differed from those originally reported by Martinac and Cui (Martinac *et al.*, 1987; Cui *et al.*, 1995). A detailed comparison revealed that MscK is activated at slightly lower tensions than MscS (Li *et al.*, 2002); however the primary distinction between the two channels lies in their kinetic behavior and regulation. With symmetrical KCl on both sides, MscK exhibits sustained activity in the entire range of activating pressures, whereas under mechanical stimulation below saturating levels, MscS response was transient with characteristic inactivation (Levina *et al.*, 1999; Akitake *et al.*, 2005). Both Martinac and Cui used constant pressure stimuli held for extended durations, conditions at which MscS populations inactivate quickly. MscK was found to be critically dependent on the monovalent cation species present in the recording solution showing activity only when K^+, NH^{4+}, Rb^+, or Cs^+ was present in the periplasmic medium and inactive when replaced with Na^+ or Li^+ (Li *et al.*, 2002). In contrast, MscS activity was demonstrated to be the same in both Na^+ and K^+ buffers (Li *et al.*, 2002; Akitake *et al.*, 2005). The channel population studied by Martinac showed marked changes in activity becoming harder to open with faster kinetics in Na^+ buffers. Cui *et al.* also studied the RQ2 strain of *E. coli* and noted that in this mutant *MscS-like* channel activity displayed a lowered opening threshold. RQ2 was later found to harbor a missense gain-of-function (GOF) mutation in the *mscK* (formerly *kefA*) gene (McLaggan *et al.*, 2002). The position of the RQ2 GOF mutation (G922S) was mapped to the gate region in the most C-terminal TM span of MscK (equivalent to the A106 position in the TM3 helix of MscS). Finally, it has been shown that the opening transition in MscS is not affected by voltage (Vasquez and Perozo, 2004; Akitake *et al.*, 2005; Nomura *et al.*, 2006).

From these comparisons, it is now evident that the early phenomenology of *MscS-like* channels in *E. coli* as reported by Martinac and Cui belongs primarily to MscK, not MscS.

C. *Purification and Reconstitution of MscS Showed Homo-Multimeric Channels Activated by Tension in the Lipid Bilayer*

After the sequence became available, the *mscS* gene was amplified by PCR and the coding sequence was modified with a 6-His tag on its C-terminus (Sukharev, 2002; Nomura *et al.*, 2006). The position of this tag was shown to have minimal effects on channel function under normal ionic conditions (Koprowski and Kubalski, 2003). The protein expressed in *E. coli* was purified on an Ni-NTA column and appeared homogeneous. When subjected to size-exclusion chromatography in the presence of β-octylglucoside and lipids, the protein emerged as a 200-kDa particle, apparently representing a stable complex. In the presence of detergent only, the complexes degraded to 30-kDa monomers. Cross-linking experiments with the bifunctional reagent DSS suggested that at least six identical subunits form the active complex.

Reconstitution of pure MscS into liposomes revealed fully active channels characterized with a weak anionic preference, slight inward rectification, and essentially nonsaturable conductance (Sukharev, 2002). Imaging of large liposome patches, along channel recording at different pressures, permitted determination of the radii of patch curvature and in such the magnitude of tension acting on channel population from the law of Laplace. The midpoint tension for MscS activation was found near 5.5 dyne/cm, in good correspondence with previous measurements by Cui and Adler (1996) performed in the whole-protoplast recording mode. In the same way that the slope of the conductance vs voltage (G–V) curve for a voltage-gated channel gives an estimation of the gating charge, the slope of P_o/P_c on tension estimates the in-plane area change of a mechanosensitive channel. Treatment of dose-response curves (Fig. 2C) in a two-state Boltzmann approximation (Sachs and Morris, 1998) predicted a protein expansion of $\Delta A = 8.4$ nm^2 and an energy difference between the closed and open conformations, in the absence of tension, of $\Delta E = 11.4$ kT. Independently conducted reconstitution experiments by Okada *et al.* (2002) confirmed that MscS is gated directly by tension in the lipid bilayer.

IV. STRUCTURAL AND COMPUTATIONAL STUDIES

A. *Structure of MscS and First Hypotheses About Its Gating Mechanism*

Successful crystallographic work by the Rees group solved the structure of MscS to 3.9-Å resolution (Bass *et al.*, 2002) revealing a homoheptameric complex with three TM helices (TM1–TM3) per subunit and a large hollow

C-terminal domain in the cytoplasm (Fig. 1). TM1 and TM2 are bundled together and splayed at about 30° relative to the axis of the pore. Due to the splay, a characteristic crevice is seen on the cytoplasmic side, between the TM1–TM2 pair and the pore-forming TM3. The TM1–TM2 assembly resembles the "paddle" of KvAP's voltage sensor (Strop *et al.*, 2003) and, due to the presence of several arginines in its structure, was proposed to function similarly as the voltage-sensitive domain for MscS. The third TM helices, TM3s, line a relatively wide but very hydrophobic pore, which after a visual inspection was deemed to be in the open conformation (Bass *et al.*, 2002). The adjacent TM3s are tightly packed through characteristic juxtaposition of conserved glycines (101, 104, and 108) and alanines (98, 102, and 106). Two rings of leucines, 105 and 109, form the narrow constriction assigned as the gate. A number of positively charged residues are situated in the pore

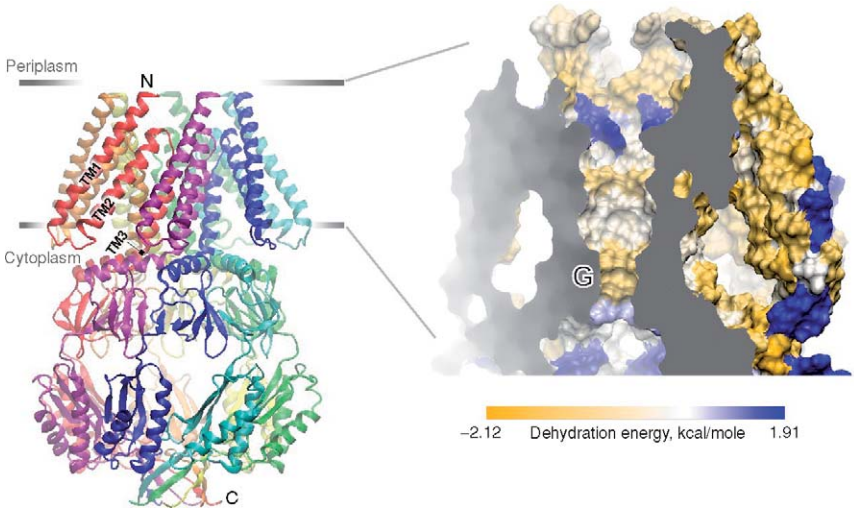

FIGURE 1 The crystal structure of MscS (left) (1MXM.pdb) and a vertical slice through the TM domain shown in a space-filled representation (right). The three membrane-spanning helices from each subunit comprise the TM domain; approximate positions of membrane boundaries are shown as horizontal lines. A large hollow domain is formed by the C-terminal domains of each subunit in the cytoplasm. On the magnified image of the TM domains, the solvent-accessible surfaces are colored according to the specific desolvation energy (from Wesson and Eisenberg, 1992). The most hydrophobic areas are yellow and most hydrophilic are blue. Averaging of solvation parameters and mapping was performed using HISTAN (www.life.umd.edu/biology/sukharevlab/download.htm#HISTAN). The pore with the hydrophobic gate (G) is formed by seven TM3 helices contributed from each subunit. A deep hydrophobic crevice separates the TM3 barrel from the peripheral TM1–TM2 helices. This crevice, likely filled with detergent in the crystals, may not exist in the native state.

vestibules (R88, K169) and were identified as candidate residues to confer the slight anionic selectivity of the channel as observed in experiments (Sukharev *et al.*, 1993; Li *et al.*, 2002; Sukharev, 2002). An unusual feature of the TM3 helices is that they are quite long and break at L111, near residue G113. The stretch of TM3 beyond the kink lies almost parallel to the membrane plane. After TM3, the polypeptide continues with the middle β-folded domain shaping the upper hemisphere of the cytoplasmic "cage." This is followed by the C-terminal domain, which forms the "bottom" of the cage. The cage is perforated by seven equatorial portals and one axially positioned "crown" hole. The structure of 26 N-terminal residues residing on the extracellular side was unresolved.

Rees and coauthors proposed that the crystal conformation of MscS represented the open state of the channel. A rough estimation of conductance using the HOLE program (Smart *et al.*, 1996) deemed that the structure could satisfy the observed ~1-nS conductance. However, later estimations predicted the need for at least an ~16-Å pore (surface-to-surface diameter) to maintain such a high current (Anishkin and Sukharev, 2004). In reference to early work by Martinac (Martinac *et al.*, 1987), the authors proposed that tension and depolarization worked synergistically to cause the upward splay of the TM1-TM2 bundle, a motion that was associated with channel opening. The closed state, correspondingly, had to be more compact structure and have a narrower pore. The authors did not exclude the possibilities of kinking or asymmetric packing of the TM3 helices to achieve complete closure (Bass *et al.*, 2002).

More recent studies have identified hypothetical conformations for the TM domains that are more compact than the crystal structure. Cross-linking experiments have identified pairs of cysteines which were shown to form disulfide bridges in the resting state, while in the crystal structure they appear to be too distant to interact (Miller *et al.*, 2003b; Edwards *et al.*, 2004). On the basis of the idea of a more compact closed state, Booth and coworkers proposed a tighter packing of the TM3 helices in the resting state; these ideas will be discussed below (Edwards *et al.*, 2005).

B. Computational Studies of MscS

1. How Compact Is the Resting State of MscS?

The solved crystal structure provided a solid starting point for the modeling of gating transitions in MscS. The first systematic attempt to envision MscS gating was a collaborative effort between the Booth, Blount, and Bowie groups which combined experimental analysis of pore mutants with Monte-Carlo (MC) optimization of the pore domain (Edwards *et al.*, 2005).

Relying on the initial assumption that the crystal structure of the TM3 bundle represents the open state (Bass *et al.*, 2002), the authors presented a model of a narrower conformation held together by tighter interhelical interactions. These low-energy conformations were obtained by searching for homodimers of the 16-residue TM3 segments. The best pairs were then duplicated around the sevenfold symmetry axis to create a heptamer. The resultant "closed" conformation, when compared with the crystal structure, suggested that tightening of the bundle could be achieved by decreasing the tilts of the TM3 helices and by slight rotation, permitting more optimal packing of alanine side chains in the complimentary groves between the conserved glycines. The new structure deviated from the crystal conformation by 1.8-Å root mean square deviation (RMSD), however the energy gain and gradient for the transition was not presented, thus making estimation of the distribution in the ensemble of similar conformations around this minimum difficult. In addition, this new "closed" structure, although very plausible, has not been tested for stability in the context of the entire TM assembly. The "closing" of the pore reduced the diameter of the hydrophobic constriction to about 2 Å making the pore certainly nonconductive. The expansion of the pore toward the crystal structure (6.5 Å in diameter) gaining about 0.3 nm^2 in cross-sectional area was deemed sufficient to achieve the observed 1-nS open-state conductance (Edwards *et al.*, 2005). It must be reiterated, however, that this hypothetical transition rests on the assumption that crystal structure is the open conformation. More recent studies suggest that even if the crystal conformation represents a native state it would likely be nonconducting.

2. The Pore as Predicted by the Crystal Structure Is Largely Dehydrated

Analysis of the pore lining indicated that L105 and L109 form not only the narrowest but also the most hydrophobic region of the MscS pore (Anishkin and Sukharev, 2004). These two "gate-keeping" residues also happen to be the most conserved residues in the larger family of MscS-type channels. The outer chamber (periplasmic side) adjacent to the gate is 12 Å in diameter and was also found to be predominantly hydrophobic.

The diameter between opposite solvent-accessible surfaces in the constriction of the crystal structure was measured to be about 6.5 Å. Estimation of the pore conductance, in continuum approximation with Hall's equation (Hall, 1975; Hille, 1992), gave a value of 70 pS, one order of magnitude less than the observed open-state conductance for MscS. In order to satisfy the observed 1-nS conductance, it was necessary to increase the effective diameter of constriction to about 16 Å. These results, which resembled dewetting transitions in hydrophobic capillaries (Beckstein *et al.*, 2001; Beckstein and Sansom, 2003) and nanotubes (Hummer *et al.*, 2001), prompted further investigation of

water's behavior in the suspiciously hydrophobic MscS pore. Analysis of the pore lining using the GETAREA protocol (Fraczkiewicz and Braun, 1998) and atomic solvation energies of Wesson and Eisenberg (1992) allowed for the calculation of the hydration energy profile along the pore axis (Fig. 2) and an assessment of the thermodynamic possibility of dehydration. A dewetting event was represented as an imaginary break in the water column filling the channel, thus creating a small "vapor plug" in the constriction. The movements of the upper and lower water surfaces decrease the contact with the protein surface, but at the same time increase the size of the water–vapor interface. Maintaining these surfaces is more energetically costly than water's contact with hydrophobic protein (surface tension of air–water interface is 72 dyne/cm = 17.7 kT/nm^2). Calculation of the energy difference for the water–vapor (w_{wv}) and water–protein (w_{wp}) boundaries produces the interfacial free energy for dewetting: $w_{dw} = w_{wv} - w_{wp}$. By finding the minima for w_{dw} in each half of the pore (Fig. 2), the positions of the water–vapor boundaries were predicted.

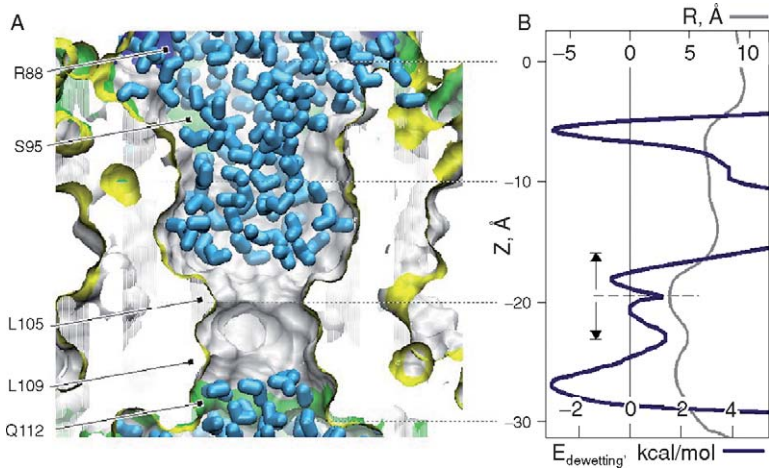

FIGURE 2 Capillary dewetting and hydration properties of MscS pore. (A) The cross section of the central pore region with its solvent-accessible surface (probe $r = 1.4$ Å) colored according to the residue type: acidic (*red*), basic (*blue*), polar (*green*), and nonpolar (*white*). Positions of residues defining the polarity of pore lining are indicated. Water molecules (*cyan*) do not occupy the constriction displaying characteristic dewetting. The coordinates are from the final frame of 6-ns molecular dynamics simulation (Anishkin, Sukharev, 2004). (B) Effective pore radius R (gray curve) and free energy of dewetting (blue curve; computed with surface tension parameter $\sigma = 20$ mJ/m^2 suggested for confined water) as functions of z coordinate. The initiation of the vapor phase formation was inferred to occur in the narrowest part of the pore (dashed line).

Equilibrium MD simulations of the MscS pore filled with flexible TIP3P water confirmed that irrespective to the initial configuration (water–filled or empty pore), the hydrophobic constriction of the crystal structure stays dehydrated most of the time and that the boundaries reflect the predicted minimums of w_{dw} (Fig. 2, blue line). The wider outer chamber of the pore also displayed a tendency to dewet when the electrostatics calculation protocol in simulations was changed from particle mesh Ewald (PME) to cutoff. Statistical treatment of trajectories showed not only lower density but also lower hydrogen bonding of water during infrequent visits into the constriction. Steered passages of Cl^- through the pore consistently produced partial dehydration of the ion and required a force of 200–400 pN to overcome an estimated barrier of 10–20 kcal/mole, implying negligibly low conductance. Importantly, MD simulations showed that the pore of the L109S GOF mutant (shown to have a low activation threshold and fast kinetics in experiments) was always fully hydrated. From these data it was concluded that the crystal structure of MscS does not represent an open state (Anishkin and Sukharev, 2004).

3. Expansion Is Required to Promote Pore Hydration and Conduction

Dewetting transitions in the MscS pore were independently observed by Sotomayor and Schulten (2004). In their study, not a segment but the complete crystal structure was embedded in the fully hydrated lipid bilayer and simulated with and without applied membrane tension. The conformation with the protein backbone harmonically restrained near the crystal coordinates displayed a dehydrated constriction most of the time with intermittent water permeation events. Without restraints, the TM domain quickly collapsed in an asymmetric occluded conformation without water inside. Application of tension (20 dyne/cm) and release of restraints resulted in a gradual expansion of the pore accompanied with increased water occupancy. The effective radius of the pore constriction during these simulations increased only minimally and events of ion permeation through the channel have not been observed. Specific interactions were noticed between charged residues residing at the ends of the TM helices and those on the cytoplasmic "cage" during evolution of the system.

Not satisfied with the conductance estimations obtained in their first rounds of simulations, Sotomayor *et al.* (2006) turned to a Boltzmann Transport Monte-Carlo method. This technique, utilizing coarse-grained representation of molecules, is capable of simulating considerably longer trajectories up to 5 μs (van der Straaten *et al.*, 2005). The restrained crystal structure again produced very low conductance. However, new expanded conformations, obtained through steered all-atom simulations (with pore constrictions as wide as 16 Å), gave conductance estimations close to the

experimentally observed 1 nS. The only inconsistencies in the simulations when compared to experiments were high anionic selectivity ($P_{K^+}/P_{Cl^-} \sim 0.1$ vs experimentally observed $P_{K^+}/P_{Cl^-} \sim 0.7$) and an opposite direction of rectification. One possible explanation is that in the simulations pore expansion was achieved by applying not only lateral tension to the entire simulation cell but also outward forces to the TM helices, the result was that only the constriction showed substantial movement. The charge-carrying vestibules remained in the crystal-like conformation, which would confer high Cl^- selectivity. This property was illustrated in analysis of the patterns of ion distributions and detailed maps of electrostatic potential across the entire protein, including the cage domain. The largest impediment to cation permeation appeared to be positive potential from the ring of Arginines 88 in the outer vestibule and from Lysines 169 inside the cage. The potential in the entire pore was very positive. The absence of the unresolved N-terminal domains may have also contributed to the electrostatic imbalance since there are three additional acidic residues (E2, D3, and D8) that, in combination with the protonated N-terminus, would result in two extra negative charges per subunit. Despite getting the constriction diameter right, the authors apparently did not achieve a true open-state conformation for the more peripheral parts of the protein. Nevertheless, one interesting change in the inner pore vestibule was observed: in the course of steered pore expansion, the characteristic kinks at G113 showed a tendency to straighten, hinting at the possible conformation of the TM3 helices in the open state (Sotomayor *et al.*, 2006).

In the very latest assessment of the conducting properties of the MscS crystal structure, Vora *et al.* (2006) performed Brownian Dynamics simulations on both the whole MscS complex and the isolated TM region. The crystal conformation of the pore produced at best ~30-pS conductance. When the constriction was expanded by 2.5 Å, the authors observed an increase in current corresponding to 0.2 nS. From this data, it was concluded once again that the crystal structure does not represent the open state of the channel.

It is known that high-electric fields promote formation of aqueous pores in low-dielectric membranes (Chernomordik *et al.*, 1987). Previous MD simulations indicated that high voltage applied across the membrane causes filling of preexisting hydrophobic pores with water (Dzubiella *et al.*, 2004) and readily creates electropores in the lipid bilayer (Tieleman *et al.*, 2003). An attempt to probe the crystal structure not by tension, but by high voltage, was published by the Dougherty group (Spronk *et al.*, 2006). Performed with the Gromos force field and SPC water, these simulations well reproduced both the dewetting events and the collapse of an unrestrained TM domain into an asymmetric occluded state as previously observed in CHARMM simulations with a TIP3P water model (Sotomayor and Schulten, 2004). Application of TM voltages

ranging from ±220 to ±1100 mV produced a moderate expansion of the pore and higher water occupancy. Importantly, it was observed that either sharpening or straightening of the kink near G113 accompanied the both asymmetric collapse and sporadic outward movements of the pore-forming TM3 helices. The authors also found that the distribution of charges in the peripheral TM domains (TM1 and TM2) strongly influence the occupancy of pore with water apparently through long-distance electrostatic interactions. At low and moderate potentials, the pore was found impermeable to ions. Under extreme TM potentials (±1100 mV), when the pore area expanded approximately two times comparing to the crystal conformation, ion permeation events were observed, with the frequency corresponding to ~0.75-nS conductance. An outward rectification manifested as higher rates of inward Cl^- permeation were observed under depolarizing conditions. In addition, the frequency of permeation events, defining the net current, was practically independent on the bulk concentration of carrier ions, which the authors' interpreted as a diffusion-limited regime. It was proposed that because the "hydrophobic lock" in the pore "disappears" with voltage, the crystal structure must resemble more the open state than the closed. These computational data, although interesting, predict a sharply nonlinear *I–V* curve with essentially zero conductance at low potentials, saturation in high salt, high anionic selectivity, and strong inward rectification. All of these findings occur in stark contrast to the entire experimental phenomenology known for the conductive state of MscS described below (Li *et al.*, 2002; Sukharev, 2002; Akitake *et al.*, 2005).

It appears that none of the existing models of the open state exactly predict the conductive properties of MscS or account for the physical expansion of the protein in the plane of the membrane, as defined by the slope of MscS activation with tension, observed in experiments. In order to be "accurate," any structural hypothesis on the functional states of the channel and/or the character of its transitions must take into account the body of experimental data regarding the conduction, activation and kinetic behavior of MscS which will be detailed below.

V. FUNCTIONAL PROPERTIES OF MscS

A. MscS Conduction and Selectivity

Despite its high conductance, which signifies substantial conformational changes in the multimeric protein, the onset of MscS conductance is extremely rapid and cooperative. An effort by the Lester group that employed high-bandwidth recording to resolve the time course of conductance change

in MscS from the closed to the fully open level revealed that most of the opening and closing events are straight transitions faster than 3 μs (Shapovalov and Lester, 2004). The recording system detected occasional substates at 2/3 of the full-open conductance.

In the open state, the current–voltage (*I–V*) relationship of MscS is almost ideally linear near 0 mV with the conductance of the channel remaining constant up to −80 mV. At positive membrane potentials, MscS current decreases due to mild inward rectification. Beyond +40 mV the presence of subconducting states were found to further reduce the effective channel conductance. Independent measurements showed that under a threefold concentration gradient of KCl, the *I–V* curve of MscS shifts by 5–8 mV toward the reversal potential for Cl^- (Li *et al.*, 2002; Sukharev, 2002). According to the Goldman equation, a 5-mV shift under such conditions corresponds to P_{K^+}/P_{Cl^-} of 0.68. Channel conductance was found nonsaturable up to 1.5-M KCl. The strictly linear dependence of the unitary conductance on the specific conductivity of bathing electrolyte, with a space constant of 3.74×10^{-8} cm, strongly suggested bulk-like conditions for ion movement in the water-filled pore (Sukharev, 2002). MscS conduction in NaCl-based buffers was found to be very similar to that in KCl (Akitake *et al.*, 2005) and the specific permeability characteristics of MscS to other ions have not been studied. The conducting properties and selectivity of MscS *in situ* (in its native setting) are practically indistinguishable from those in reconstituted patches (Sukharev *et al.*, 1993; Li *et al.*, 2002; Sukharev, 2002).

B. Gating Characteristics of MscS In Situ

The study by Akitake *et al.* (2005) was the first to employ a high-speed pressure clamp apparatus to deliver reproducible pressure stimuli to WT MscS populations. Expression of MscS in a background free of other mechanosensitive channels [MJF465; triple *mscS*-, *mscK*-, *mscL*-knockout strain (Levina *et al.*, 1999)] gave robust responses with up to 100 channels in an excised patch. WT MscS channels steeply activate with pressure and remain stably open in cases of constant saturating pressure. However, at subsaturating pressures MscS inactivates and is unable to respond to subsequent stimuli immediately. It takes about 3 min at zero tension and voltage for the population to completely return from the inactivated, back to the resting state. The open dwell time for WT MscS depends on tension, but near the activation threshold, the distribution peaks around 100–150 ms (Edwards *et al.*, 2005; Akitake, unpublished data).

An analysis of MscS population responses to linear ramps of negative pressure, after rescaling pressure to tension [the midpoint pressure $p_{1/2}$ corresponds to a membrane tension of 5.5 dyne/cm (Sukharev, 2002)], yielded the thermodynamic parameters of $\Delta E = 24$ kT, $\Delta A = 18$ nm^2 as estimates of the energy and in-plane area changes associated with the opening transition. These values, extracted from MscS activities in native membranes, were higher than those reported from studies in liposomes ($\Delta E =$ 11.4 kT and $\Delta A = 8.4$ nm^2). The larger ΔA and ΔE in the former case may be a result of the different stimulus protocols applied. In the liposome-reconstitution experiments, dose-response curves were measured using a series of descending steps (under more reversible conditions). It now appears that the ascending pressure ramp regime, even with slow ramps, may be different from the descending regime. A comparison of WT MscS traces recorded with symmetric linear ascending and descending ramps of pressure showed clear hysteresis, indicating that the opening and closing transitions are characterized with different slopes on tension and are likely to proceed through different transition states (Akitake *et al.*, unpublished data). Responses to just the descending ramps produced estimates for ΔA between 9 and 12 nm^2, more consistent with the previous data obtained in liposomes (Sukharev, 2002). Another factor that may affect the apparent slope of $P_o(\gamma)$ is the uniformity of channel population (Chiang *et al.*, 2004). The higher slope and respectively larger apparent ΔA suggest that the channel population in native patches is more uniform (in terms of ΔE and/or local tension) compared to liposome patches. The nonhomogeneity of MscS channels in liposomes could potentially arise from lateral clustering. It also cannot be excluded that liposome and spheroplasts patches, when stressed with steady pressure gradients, exhibit different TM distributions of lateral tension. Indeed, in liposome patches, tension may be more concentrated in the pipette-attached monolayer due to unrestrained slippage and relaxation of the opposite monolayer in the low-protein membrane. If MscS expansion is nonuniform along the z-axis, redistribution of tension along the same axis would lead to changes in the apparent expansion area in the x–y plane. Currently there is no reason to believe that MscS in native membranes expands more, or gates very differently compared to liposomes.

In sharp contrast to the early phenomenology (Martinac *et al.*, 1987), it was found that MscS exhibits essentially voltage-independent activation by tension. The responses of channel populations to linear pressure ramps at different voltages (from +100 to −100 mV) showed no significant shift in the pressure midpoint of activation. The slope of ΔE plotted as a function of voltage, produced the gating charge of $q = +0.8$ e per channel complex or about +0.1 e per subunit signifying that activation is not associated with any significant transfer of charge across the membrane.

The process of MscS activation was found to be influenced by high-molecular-weight compounds such as ficoll or polyethylene glycols (PEGs) present on the cytoplasmic side of the membrane (Grajkowski *et al.*, 2005). The right-shift of activation (P_o—pressure) curves was more pronounced (~30%) in the presence of a high-molecular-weight PEG (6.0 kDa), apparently impermeable through the fenestrations in the cytoplasmic cage, and a much smaller shift was observed with a smaller PEG (0.2 kDa). Both small and large PEGs were found to be inhibitory for MscS channel populations, though the exact mechanisms of their action appear to be different.

C. Mutations That Affect MscS Activity

The V40D/G41S mutation was first isolated in a random mutagenesis screen (Okada *et al.*, 2002) as it resulted in a GOF phenotype inhibiting bacterial growth in liquid culture on induction. Further analysis revealed that V40D alone produced the GOF phenotype and since this hydrophobic-to-charged substitution mapped to the first TM domain, it was inferred that TM1 might line the conducting pore of MscS (Okada *et al.*, 2002). In later experiments, three growth-suppressing mutations, previously identified in the *mscK* locus of *Salmonella typhimurium*, were replicated into MscS and found to confer visible GOF phenotypes (Miller *et al.*, 2003a). Two of these mutants T93R and L109S were severe GOFs, whereas the third mutation, G108S, displayed a milder phenotype. Unlike the V40D mutation, these substitutions mapped to TM3, suggesting that TM3, not TM1, is the pore lining helix. Solution of the crystal structure in 2002 confirmed that TM3 lines the pore, with the T93 residue mapped to the short loop connecting TM2 with TM3 and the residues G108 and L109 right in the gate. The substitution L109S in the most severe GOF mutant was predicted to remove part of the hydrophobic lock that keeps MscS closed.

Guided by the crystal structure, Booth and coworkers generated a number of substitutions, which hypothetically affected the packing of TM3 helices in the pore of MscS. It was found that complimentary TM3–TM3 interfaces play a pivotal role in setting the threshold for MscS activation. Replacement of conserved glycines with alanines in this region (G101A, G104A, and G108A) produced MscS channels with higher activation thresholds, closer to that for MscL. These ''stiffening'' effects were partially reversed by making reciprocal substitutions on the neighboring surface (A106G/G108A and A106G/G104A). The authors concluded that substitution of the glycines with alanines created artificial ''knobs'' on the surface of the mutated TM3s. These ''knobs'' sterically clash with the existing alanine ''knobs'' on

the opposite interhelical face, thus creating a higher barrier for the opening transition. While this mechanism is plausible, the authors did not consider the relationship between the polarity of substitutions and the activation thresholds, limiting discussion to the steric aspect of the interhelical interactions (Edwards *et al.*, 2005). Their own analysis of G101S and G108S, hydrophilic mutations that should also produce steric conflicts, revealed channels that were easily opened. Conversely, hydrophobic and bulkier substitutions A98L, A106V, A106L produced extremely "stiff" channels. It now appears that hydration effects have a stronger contribution to the activation threshold than the steric effects (Anishkin and Sukharev, 2004; Akitake *et al.*, unpublished data).

D. MscS Inactivation

1. Parameters Affecting the Rate of Inactivation

Inactivation is one of the most intriguing features of MscS gating. The effects of MscS inactivation appear to be reversible in native membranes and largely irreversible in liposomes (Sukharev, 2002). Typical MscS activity in response to a fast pressure stimulus, which is then held at a constant nonsaturating level, is a spike of conductance followed by decay due to inactivation (Levina *et al.*, 1999; Akitake *et al.*, 2005). Koprowski and Kubalski (1998) were the first to characterize time-dependent inactivation/adaptation and recovery of MscS-like channel populations. It was found that the inactivation/adaptation time constant τ was dependent on the magnitude of pressure application. It was also noted that adaptation was insensitive to voltage at moderate ($\pm$30 mV) potentials (Koprowski and Kubalski, 1998). In a following study of the inactivation process, populations of MscS were stimulated with reproducible pulses of pressures under a wider ($\pm$100 mV) range of voltages (Akitake *et al.*, 2005). The data shows that low-activating pressures promoted visible inactivation at hyperpolarizing (positive pipette) voltages, a process that was sped up by more than an order of magnitude under depolarizations beyond 40 mV. Higher depolarizing voltages were able to drive the MscS population to an inactivated state even when stimulated by previously saturating pressures. Furthermore, it was noticed that subjecting the channel population to depolarizing voltages increased the frequency of channel transitions to subconducting states (Akitake *et al.*, 2005). High-resolution recordings of MscS at high voltage identified several subconducting states (Shapovalov and Lester, 2004). These observations are consistent with the notion that substates are intermediates between the open and inactivated states and entering a substate predisposes MscS channels to inactivation.

The involvement of the C-terminal domain of MscS in the inactivation process is an area of active study. The crystal structure of MscS identified several charged residues along TM1, TM2, and TM3, which were designated as putative voltage sensors (Bass *et al.*, 2002; Spronk *et al.*, 2006). Nomura *et al.* (2005) mutated each of these residues and discovered that the voltage-sensitive characteristics of MscS inactivation were unchanged. Deletion studies have revealed that almost the entire C-terminal domain of MscS is required for proper channel assembly (Miller *et al.*, 2003a). Study was conducted on a mild C-terminal truncation mutant (Δ266–286) in which the sevenfold β-barrel forming the base of the cytoplasmic cage was removed. This mutant was able to incorporate into the membrane but displayed greatly reduced activity and a striking inability to recover from inactivation (Schumann *et al.*, 2004). The involvement of the C-terminal domain in MscS inactivation and recovery was initially demonstrated by Koprowski and Kubalski (2003) in cross-linking experiments targeting multiple lysines concentrated in cage region. Later, the same group (Grajkowski *et al.*, 2005) noticed that large-molecular-weight cosolvents, when added from the cytoplasmic face, had a marked effect on MscS inactivation. Data collected with PEGs of various sizes showed that smaller molecular weight PEGs, those that presumably penetrate the C-terminal cage and make their way to the gate, tended to reduce channel conduction. However, larger PEGs did not appear to affect conduction, rather their presence increased the rate of MscS inactivation. Interpreted as a "cosolvent" effect, the inactivation-promoting action of PEGs could be linked to pressures across the wall of the cage and structural changes in the C-terminal domain of MscS (Grajkowski *et al.*, 2005). These findings implicate a critical role of the C-terminal in the process of inactivation.

2. MscS Activity Depends on the Rate of Pressure Application

Unlike MscL, the activity of MscS is strongly dependent on the rate of stimulus application. MscS populations were stimulated with ramps of pressure that linearly increased from zero to a saturating value over varying time span (i.e., with rates from 2.7 to 240 mm Hg/s). It was found that the midpoint activation pressure remained fixed; however, it was obvious that the activity (maximal conductance) at the end of the ramp was higher with steeper ramps (Akitake *et al.*, 2005). With the slowest ramp tested, only ~30% of the MscS population was shown to activate. Inactivation may play a critical role in this effect as reduction of maximal current was observed to be much stronger at depolarizing voltages (beyond 40 mV). To obtain further insight into this phenomenon, a two-step protocol was employed in which a longer prepulse was delivered to trigger activation (with concomitant inactivation), and a subsequent shorter step of saturating pressure

applied to test the availability of the active population. Kinetics of the recorded currents indicated that inactivation was faster at intermediate pressures where only a portion of the MscS population activates (Akitake *et al.*, 2005). This was consistent with earlier inactivation studies that showed a tension dependence of the rate of inactivation (Koprowski and Kubalski, 1998). It was found that the rate of inactivation was greatest in a narrow range of pressures just above the opening threshold and below the activation midpoint of the MscS population. When MscS is subjected to a slow ramp of pressure, the channels spend more time in this window of pressures that promote channel inactivation resulting in lower final conductance of the population. This interplay of opening and tension-dependent inactivation permits MscS to respond in full to an abrupt stimulus and ignore stimuli applied slowly as if the gate of the channel is connected to the tension-transmitting element effectively via a velocity-sensitive "dashpot" (Akitake *et al.*, 2005). This functional design allows the channel to adapt to mild or slow-onset osmotic shocks, when collapse of membrane potential and indiscriminate release of ions and small osmolytes may not be desirable.

3. Small Amphipathic Compounds Promote MscS Inactivation and Subunit Separation

Early studies revealed strong effects of small amphipathic molecules on the gating of mechanosensitive channels (Martinac *et al.*, 1990). Cationic and anionic amphipathic compounds, such as chlorpromazine (CPZ) and trinitrophenol (TNP), when added to the bath solution in excised patch-clamp recordings did not appear to bind to the channels directly, but lowered the activation threshold pressure for the population presumably due to curvature and/or area stress in the surrounding lipid bilayer (Sheetz and Singer, 1974; Markin and Martinac, 1991). Since then membrane-active amphipathic substances, such as lysophosphatidylcholines (LPCs), have been used to shift the state equilibrium in MscL, especially when applied asymmetrically (Perozo *et al.*, 2002).

Short-chain alcohols are different from typical amphipaths as they are smaller and act on membranes in higher concentrations, as cosolvents (Barry and Gawrisch, 1994; Koenig and Gawrisch, 2005). 2,2,2-Trifluoroethanol (TFE) is a low-dielectric solvent that has known, since the 1960s, to strongly affect protein structure. At high concentrations, TFE tends to stabilize the secondary structure of soluble proteins, whereas in membrane proteins the effects are mainly destabilizing. The "inverted" design of integral membrane proteins (hydrophobic on periphery) when compared to soluble proteins (hydrophobic inside) appears to make them more susceptible to disruption by TFE. MscS was identified as one of the inner membrane proteins that

changed its oligomerization state in two-dimensional gels on exposure to TFE (Spelbrink *et al.*, 2005). Isolated MscS oligomeric complexes were shown to remain stably associated as homoheptamers and homotetramers in cold lithium dodecyl sulfate polyacrylamide gel electrophoresis (LDS-PAGE) (Akitake *et al.*, 2007). The addition of 10 vol% TFE resulted in complete dissociation of MscS into monomeric subunits. Patch-clamp analysis of MscS channels asymmetrically exposed to TFE from either the pipette or the bath showed shifts in the activation dose response curves to the left and right, respectively. These shifts are consistent with a buildup of lateral pressure due to intercalation of TFE into one leaflet of the membrane. In addition, it was found that TFE added to the bath causes reversible inactivation of the MscS population. The amount of inactivation was found to increase with greater concentrations of TFE. Fifty percent MscS inactivation was observed with a TFE concentration near 0.7 vol%. The shift in equilibrium toward the inactivated state correlated with the increased rate of MscS inactivation and slower recovery. In the presence of 0.5 vol% TFE, application of subsaturating stimulus revealed ~2.6 times quicker inactivation and ~4.2 times longer recovery compared to TFE-free control preformed in the same patch under identical conditions (Akitake *et al.*, 2007).

It appears that both, the change in state distribution at low TFE concentrations and subunit separation at higher TFE, can be explained by the same thermodynamic property of TFE to separate helices by preferential partitioning into hydrophobic protein crevices. The membrane in this case may also act as a hydrophobic reservoir for TFE increasing its concentration several fold relative to the bulk. At these concentrations, TFE would prefer to partition into the easily formed crevices between TM2 and TM3 (as depicted in the crystal structure, Fig. 1). Crevice formation may shift the channel equilibrium toward the inactivated state consistent with the idea that separation of these helices is the mechanism of inactivation (Akitake *et al.*, 2005, 2007).

VI. WHAT DO THE CLOSED, OPEN, AND INACTIVATED STATES OF MscS LOOK LIKE?

Like any other protein crystal structure, the structure of MscS represents only one of the many physical conformations for the channel. In the absence of other direct structural data, visualization of MscS's functional states (closed, open, and inactivated) can be obtained only through extensive modeling and simulations, judicious analysis of permitted conformations and interpolation of smooth transitional paths between them, and by critical

comparison of experimentally observed parameters. A "good" model must maintain consistency between each of these different types of parameters.

A. Is the Crystal Structure a Native State?

The first model of MscS gating by Bass and colleagues postulated that the crystal conformation represents the conducting state of the channel with the characteristically tilted TM1–TM2 helices signifying the voltage-driven transfer of charges previously, and erroneously, associated with MscS activation. It was also implied that the resting (nonconductive) state of the channel has less tilted peripheral helices and that packing of the central TM3 helices should be tighter. Computational data discussed above provides compelling evidence that the crystal structure of MscS is actually nonconductive under physiological voltages and thus cannot represent an open conformation. The crystal structure does not appear to represent a closed (resting) state either, as the tilted lipid-facing TM1 and TM2 helices are splayed out and make no physical contacts with the gate-forming TM3s. The absence of TM2–TM3 interactions makes it unclear how membrane stretch, received by the peripheral helices, could be transmitted to the gate. In this regard, the crystal conformation would appear to be irresponsive to membrane stretch, an attribute of the inactivated state. Likewise the diameter of the crystal pore does not satisfy the observed ~1-nS conductance for MscS (Anishkin and Sukharev, 2004; Sotomayor and Schulten, 2004; Sotomayor *et al*., 2006; Spronk *et al*., 2006; Vora *et al*., 2006), and the splaying motion of TM1 and TM2 would produce only small in-plane protein expansion (~2–3 nm^2), far short of 8–12 nm^2 deduced from the slope of MscS activation curves.

It, therefore, seems plausible that the crystal conformation, with kinked TM3 helices, may resemble the inactivated MscS channel. One major problem with the crystal conformation is that the peripheral helices TM1 and TM2 do not form a continuous lipid-facing wall, but were found to protrude outward, forming deep hydrophobic crevices, which must be filled with the detergent in the crystals. Tilting of individual TM helices in the bilayer is energetically unfavorable (de Planque *et al*., 2003; Strandberg *et al*., 2004) and the complete absence of tilt-stabilizing helical contacts between the TM1–TM2 pairs suggests that the unusual splay could be an artifact of delipidation. As previously described, independent MD simulations revealed that when the channel is embedded into lipids in its crystal conformation, the pore quickly collapses (Sotomayor and Schulten, 2004; Spronk *et al*., 2006). In this regard, as a starting conformation, the crystal structure appears to be incompatible with a typical bilayer environment. Packing of the peripheral

helices to be more parallel as proposed by Booth and coworkers (Miller *et al.*, 2003b; Edwards *et al.*, 2004) may alleviate the problem of instability; however, the sharp kink at G113 would still impose some gap between TM2 and TM3. This gap, generally hydrophobic (see Fig. 1 and legend) can be filled with small apolar substances such as TFE, which was shown to stabilize the inactivated state (Akitake *et al.*, 2007). Therefore, a conformation similar to the crystal state, but with more parallel packing of helices and smaller gaps, is proposed for the conformation of the native inactivated state.

B. Closed State

To achieve the resting (closed) conformation, an even tighter packing of the TM helices from the crystal conformation would be required (Miller *et al.*, 2003b; Edwards *et al.*, 2004). This does not necessarily mean that the TM3 barrel should be packed much tighter as well. The already tight packing and limited mobility (low β-factor) of the TM3 helices in the crystal structure is consistent with this conformation being close to an energetic minimum. If the crystal structure pore were truly nonconducting, additional packing of TM3 as proposed by Edwards *et al.*, although possible, would not be required to close MscS.

The model shown in Fig. 2 (middle) represents the results of steered simulation, in which the crystal structure (left) was subjected to uniform constricting forces. This compaction restored the TM2–TM3 contacts, but also caused straightening of the G113 kink to resolve steric conflict between the distal part of TM3 and the TM1–TM2 linker. An alternative kink was created at the highly conserved G121. Preliminary 6-ns simulations have shown that the constriction in this conformation ($\sim$5 Å in diameter) remains dehydrated and thus nonconductive. The backbone of the pore in this "relaxed" model (residues 98–110) had RMSD deviation of only 0.73 Å when compared to the crystal structure and 1.79 Å compared to the model of Edwards *et al.* (2005).

C. Open State

What does it take to arrive at the open conformation of MscS? It is thought that tension applied to the peripheral helices (TM1 and TM2) is transmitted to the central pore-lining helices (TM3) straightening them completely and producing a substantial outward expansion of the pore. This transition (Fig. 3) was achieved through a series of expansion-minimization

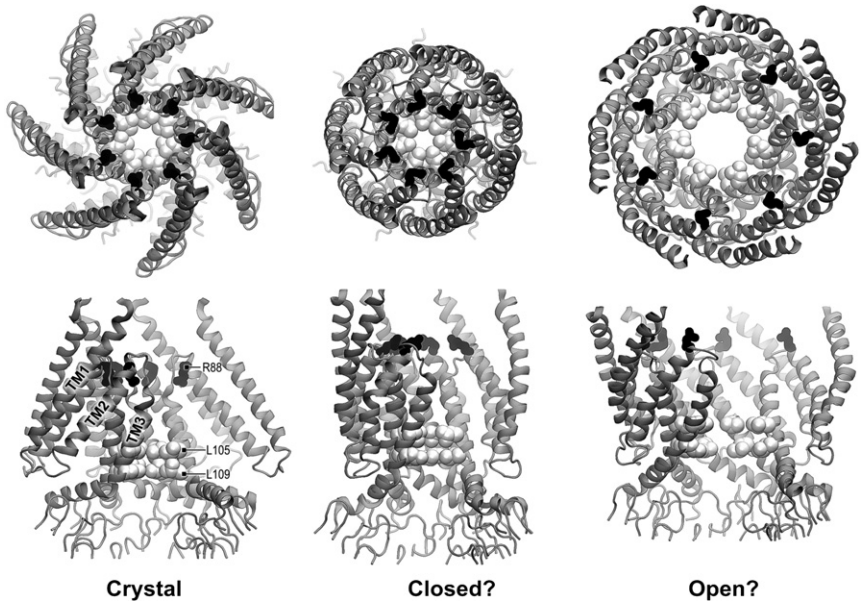

FIGURE 3 The crystal conformation of the TM domain and models of the closed and open states of MscS. Molecular structures are in the "ribbon" representation, while L105 and L109 residues forming the constriction are shown in white VDW spheres, and R88 are presented as black sticks. The two front subunits are removed for a better view of the pore interior. The first 26 N-terminal residues were unresolved in the crystal structure, are not shown in the models for consistency. Models were derived from the crystal conformation using steered molecular dynamics and targeted energy minimization in vacuum and in a fully hydrated POPC bilayer. To produce the closed state model, centripetal harmonic forces were applied to the transmembrane helices TM1 and TM2 of the crystal structure. The amplitude of the forces was gradually increased up to the minimal value when the helices moved and restored the contact with the TM3 barrel, while the secondary structure remained intact. The transition from the closed to the open state was initiated by the centrifugal forces applied to the whole transmembrane region. After the initial ~1 Å displacement, the expansion of the protein was continued by intermittent cycles of unrestrained relaxations, small (~0.2 Å) extrapolated displacements, and energy minimizations. An open conformation satisfying the experimentally measured conductance and in-plane expansion area was selected (shown as the open state model), embedded into a fully hydrated POPC bilayer and simulated without restraints for 4 ns. The simulation confirmed the stability of the model. (A. Anishkin *et al.*, in preparation).

cycles, followed by a 4-ns equilibrium simulation in the fully hydrated POPC bilayer (A. Anishkin, in preparation). The structure resolved in a stable tilted conformation of TM3s with an aqueous central lumen of about 20 Å in diameter. It was observed that a slight rotation of TM3s resulted in the gate-keeping leucines 105 and 109 swinging to the side, thus opening

conducting pathway. At the same time, rotation of TM3 fully exposed the conserved glycines 101, 104, and 108 to the lumen, a feature that dramatically increased the polarity (and wettability) of the pore surface. Exposure of these glycine residues, which are firmly buried in interhelical contacts in the resting conformation, appears to stabilize the hydrated state of the open pore. This glycine-mediated stabilization of the open conformation is highly consistent with the data presented by Edwards *et al.* (2005) who demonstrated that substitutions of these glycines to alanines (covering the polar backbone with apolar methyl) substantially increases the tension required for activation, whereas substitution with larger but more polar serines facilitates the opening transition.

In this hypothetical open conformation, the conductance of the entire channel satisfied the observed ~1 nS and the entire opening transition provided ~12 nm^2 of in-plane protein expansion consistent with that derived from MscS activation curves. The outward movement of the TM helices, which displace the charged R88 residues farther away from the pore axis, is expected to produce a moderately anion-selective channel.

Transition from the open to the inactivated state can be envisioned as a breakage of the TM3 helices at G113. Kink formation at G113 closes the pore by bringing the TM3 segments almost parallel to each other. In this conformation, the now closely associated leucine 105 and 109 residues act to expel water and cease conduction. This transition may be accompanied by a partial disengagement of TM2 from TM3 retuning the system to a crystal-like conformation. Interestingly, the kink-supporting cluster of residues, equivalent to G113-S114 in MscS, is absent in MscK, which does not inactivate under similar stimuli (Levina *et al.*, 1999).

VII. EMERGING PRINCIPLES OF MscS GATING AND REGULATION AND THE NEW DIRECTIONS

On the basis of the experimental and computational data discussed above, it appears that the gating of MscS involves cooperative entry and retraction of water from the pore. In its closed state, the hydrophobic nature of MscS's conduction path leads to a complete dewetting of the constriction (L105/L109) and possibly the outer chamber lined by A102 and A98. The formation of this vapor plug would create a tight seal that is impermeable not only to all typical inorganic ions but to protons as well. This is a critical feature of a large conductance channel because any residual water bridge would invariably create a proton leak in the cytoplasmic membrane and decouple the bacterial energetics. The effects of severe GOF mutations (L109S) are highly consistent with the permanently hydrated state of such pores making them leak.

A complete retraction of water from the pore cavity would also create meniscus-like interfaces above and below the constriction. These high-tension interfaces would stabilize the tightly packed closed conformation. One challenging future project would be direct detection of the vapor plug in MscS possibly through the use of spectroscopic or particle scattering techniques.

When tension is applied to MscS, the TM domain of the channel undergoes substantial expansion in the plane of the membrane (8–12 nm^2), moving the protein–lipid boundary outward. Simultaneous widening of the pore increases the number of polar atoms exposed to the lumen and effectively changes the character of pore lining from hydrophobic to hydrophilic. This change promotes hydration, which must precede the onset of conduction. It is important to remember that the changes of conduction from zero to the fully open level and then back to zero are sharp processes occurring in an all-or-none fashion within 3 μs (Shapovalov and Lester, 2004). These opening and closing events are significantly shorter than what would be expected for the entire transition of the bulky MscS protein involving a lateral displacement of lipids and possible cytoplasmic cage transformation (Miller *et al.*, 2003b; Edwards *et al.*, 2004). Therefore, the character of conduction change in MscS may signify critical wetting–dewetting events involving primarily the dynamics of water (not the entire protein), which in simulations occur in 1–3 ns for the preexpanded protein. An important next step in clarifying the opening and closing conformational pathways would be to carefully study the hysteresis between the two events and determine the positions of the transition states.

The characteristic kink found in the crystal structure near G113 appears to be a signature of the inactivated MscS. In contrast, the noninactivating channel MscK shows strong helical propensity at this location. Dependence of the inactivation/recovery processes in MscS to the relative helical propensity of TM3 is currently under investigation. The MscS channel displays the unique ability to undergo time- and pressure-dependent desensitization/inactivation, with the channel population responding in full to an abrupt stimulus and not to those applied slowly (Akitake *et al.*, 2005). This kinetic property of "dumping" a slowly applied force may be important in different environmental situations where dilution of the external medium occurs gradually and thus fast and indiscriminate release of osmolytes is not desirable. Turning off MscS activity under such conditions provides an opportunity for more specific transporters/exchangers to balance osmotic forces in a more selective way. One important experiment will be to compare the cellular responses of bacteria to acute and gradual osmotic changes in strains where MscS is the sole osmolyte release valve. It is possible that the presence or absence of aquaporins, which regulate the rate of water transport and

turgor pressure onset (Booth and Louis, 1999), may influence the activity of MscS.

The structural design of MscS is such that the gate-forming TM3 helix is directly connected to a large C-terminal cage domain. Deciphering the interplay between the opening and inactivation processes with the volume and/or conformation of this hollow domain is an attractive idea. It appears that the cage may function as an internal osmosensor that discriminates between the osmotic pressure created by small (permeable) osmolytes from the oncotic pressure created by large macromolecular constituents. If a substance easily penetrates the fenestrations in the cage domain, it will not contribute to a pressure gradient across the cage wall. One example is when the turgor pressure inside the cell is created primarily by inorganic ions such as K^+ during the first stage of the cellular response to hyperosmotic stress. The cage will not experience any extra pressure and the channel will open to release these extra ionic constituents and balance the osmotic gradient. However, larger macromolecules that are cage-impermeable are also too large to be expelled by MscS. If these molecules are responsible for the cellular turgor pressure, their exclusion from the cage will exert a secondary osmotic imbalance on the C-terminal domain, causing its collapse. This mechanism appears to prevent futile openings that would only destroy the membrane potential and normal ionic gradients. The cage of MscS senses the ''squeezing'' action of these high-molecular-weight osmolytes and renders the channel insensitive to membrane tension by driving the gate into an inactivated conformation. Data presented by the Kubalski group (Grajkowski *et al.*, 2005) is highly consistent with this hypothesis. Further testing of MscS responses in the presence of natural cytoplasmic constituents, other high-molecular-weight compounds and compatible osmolytes is being conducted.

In addition to being an internal osmosensor, the cage domain of MscS may also act as a voltage or ionic flux sensor. The report by Nomura *et al.* (2006) has demonstrated that the voltage dependence of inactivation remains even when most of the charges in the TM domain are neutralized by mutations. It is important to note that voltage-dependent inactivation is observed to develop only after the channel opens. It appears that high depolarizing potentials are unable to drive the closed channel into the inactivated state. These observations suggest that the ionic flux itself, and/or the accompanying elecroosmotic water flux, drives MscS into the inactivated state. Careful testing of this hypothesis is certainly required; however, preliminary data show a strong dependence of inactivation by voltage on the type of permeant ions (Akitake, unpublished data). This is consistent with the idea that the voltage sensor in MscS is not located in the membrane where it would perceive static voltage, but is more likely located intracellularly where it perceives

unbalanced ion fluxes causing coupled water fluxes and integrates this perturbation with the osmotic contributions of different solutes. It will be very interesting to see if channel activity is influenced by proline, betaine, and glutamate and ultimately whether MscS is part of the system that exchanges K^+ for compatible osmolytes during the upshock response (Wood *et al.*, 2001; Booth *et al.*, 2003).

Recent studies of MscS homologues have revealed interesting clues about the role of the small mechanosensitive channel in higher organisms. Do all MscS-type channels function in the same way? The answer is apparently not. Even the related bacterial channel MscK, which features activities similar to MscS in patch-clamp experiments, cannot by itself rescue MJF465 cells from osmotic shock. On the other hand, the recently characterized MscS homologue from *A. thaliana*, MSL3, when expressed in *E. coli*, is capable of restoring osmoprotective function (Haswell and Meyerowitz, 2006). There are yet no reports of any electrophysiological data for MSL3, and it is possible that MSL3 has a smaller conductance that is not readily seen in patch clamp. MSL3 was demonstrated to participate in chloroplast shape formation and division. Deletion of MSL2 and MSL3 resulted in chloroplasts that were much larger and swollen. A failure of this type of regulation suggests that MSLs indeed act as tension-activated release or exchange valves; however, to accomplish this function the rate of transport through these channels need not be as high as that of MscS (10^9 ions per second). From analysis of the sequence, *A. thaliana* MSLs have longer hydrophobic constrictions (three rings of bulky aliphatic residues instead of two in MscS), and this may critically change the rate of ion transport. The presence of these bacterial-type channels in *A. thaliana* and their role in chloroplasts volume regulation is a vivid illustration of how a function of initially bacterial channels was preserved and adapted in the course of endosymbiotic evolution of plastids (Haswell and Meyerowitz, 2006).

MscS is undoubtedly a high-value system for experimentation and molecular computation that will aid in the discovery of new biophysical principles of ion channel regulation. It is hopeful that the continued study of MscS will eventually link its unique and complex phenomenology to a greater understanding of the mechanisms of cellular/organellar growth, development, and flexible adaptation to various environments.

References

Akitake, B., Anishkin, A., and Sukharev, S. (2005). The "dashpot" mechanism of stretch-dependent gating in MscS. *J. Gen. Physiol.* **125,** 143–154.

Akitake, B., Spelbrink, R. E., Anishkin, A., Killian, J. A., de Kruijff, B., and Sukharev, S. (2007). 2,2,2-Trifluoroethanol changes the transition kinetics and subunit interactions in the small bacterial mechanosensitive channel MscS. *Biophys. J.* (in press).

Anishkin, A., and Sukharev, S. (2004). Water dynamics and dewetting transitions in the small mechanosensitive channel MscS. *Biophysics* **86,** 2883–2895.

Barry, J. A., and Gawrisch, K. (1994). Direct NMR evidence for ethanol binding to the lipid-water interface of phospholipid bilayers. *Biochemistry* **33,** 8082–8088.

Bass, R. B., Strop, P., Barclay, M., and Rees, D. C. (2002). Crystal structure of *Escherichia coli* MscS, a voltage-modulated and mechanosensitive channel. *Science* **298,** 1582–1587.

Beckstein, O., and Sansom, M. S. (2003). Liquid-vapor oscillations of water in hydrophobic nanopores. *Proc. Natl. Acad. Sci. USA* **100,** 7063–7068.

Beckstein, O., Biggin, P. C., and Sansom, M. S. P. (2001). A hydrophobic gating mechanism for nanopores. *J. Phys. Chem. B* **105,** 12902–12905.

Berrier, C., Besnard, M., Ajouz, B., Coulombe, A., and Ghazi, A. (1996). Multiple mechanosensitive ion channels from *Escherichia coli*, activated at different thresholds of applied pressure. *J. Membr. Biol.* **151,** 175–187.

Blount, P., Sukharev, S. I., Moe, P. C., Martinac, B., and Kung, C. (1999). Mechanosensitive channels of bacteria. *Methods Enzymol.* **294,** 458–482.

Booth, I. R., and Louis, P. (1999). Managing hypoosmotic stress: Aquaporins and mechanosensitive channels in *Escherichia coli*. *Curr. Opin. Microbiol.* **2,** 166–169.

Booth, I. R., Edwards, M. D., and Miller, S. (2003). Bacterial ion channels. *Biochemistry* **42,** 10045–10053.

Britten, R. J., and McClure, F. T. (1962). The amino acid pool in *Escherichia coli*. *Bacteriol. Rev.* **26,** 292–335.

Chang, G., Spencer, R. H., Lee, A. T., Barclay, M. T., and Rees, D. C. (1998). Structure of the MscL homolog from Mycobacterium tuberculosis: A gated mechanosensitive ion channel. *Science* **282,** 2220–2226.

Chernomordik, L. V., Sukharev, S. I., Popov, S. V., Pastushenko, V. F., Sokirko, A. V., Abidor, I. G., and Chizmadzhev, Y. A. (1987). The electrical breakdown of cell and lipid-membranes—the similarity of phenomenologies. *Biochim. Biophys. Acta* **902,** 360–373.

Chiang, C. S., Anishkin, A., and Sukharev, S. (2004). Gating of the large mechanosensitive channel *in situ*: Estimation of the spatial scale of the transition from channel population responses. *Biophysics* **86,** 2846–2861.

Csonka, L. N. (1989). Physiological and genetic responses of bacteria to osmotic stress. *Microbiol. Rev.* **53,** 121–147.

Csonka, L. N., and Hanson, A. D. (1991). Prokaryotic osmoregulation: Genetics and physiology. *Annu. Rev. Microbiol.* **45,** 569–606.

Cui, C., and Adler, J. (1996). Effect of mutation of potassium-efflux system, KefA, on mechanosensitive channels in the cytoplasmic membrane of *Escherichia coli*. *J. Membr. Biol.* **150,** 143–152.

Cui, C., Smith, D. O., and Adler, J. (1995). Characterization of mechanosensitive channels in *Escherichia coli* cytoplasmic membrane by whole-cell patch clamp recording. *J. Membr. Biol.* **144,** 31–42.

de Planque, M. R., Bonev, B. B., Demmers, J. A., Greathouse, D. V., Koeppe, R. E., Separovic, F., Watts, A., and Killian, J. A. (2003). Interfacial anchor properties of tryptophan residues in transmembrane peptides can dominate over hydrophobic matching effects in peptide-lipid interactions. *Biochemistry* **42,** 5341–5348.

Dzubiella, J., Allen, R. J., and Hansen, J. P. (2004). Electric field-controlled water permeation coupled to ion transport through a nanopore. *J. Chem. Phys.* **120,** 5001–5004.

Edwards, M. D., Booth, I. R., and Miller, S. (2004). Gating the bacterial mechanosensitive channels: MscS a new paradigm? *Curr. Opin. Microbiol.* **7,** 163–167.

Edwards, M. D., Li, Y., Kim, S., Miller, S., Bartlett, W., Black, S., Dennison, S., Iscla, I., Blount, P., Bowie, J. U., and Booth, I. R. (2005). Pivotal role of the glycine-rich TM3 helix in gating the MscS mechanosensitive channel. *Nat. Struct. Mol. Biol.* **12,** 113–119.

Epstein, W. (2003). The roles and regulation of potassium in bacteria. *Prog. Nucleic Acid Res. Mol. Biol.* **75,** 293–320.

Ferguson, G. P., Battista, J. R., Lee, A. T., and Booth, I. R. (2000). Protection of the DNA during the exposure of *Escherichia coli* cells to a toxic metabolite: The role of the KefB and KefC potassium channels. *Mol. Microbiol.* **35,** 113–122.

Fraczkiewicz, R., and Braun, W. (1998). Exact and efficient analytical calculation of the accessible surface areas and their gradients for macromolecules. *J. Comput. Chem.* **19,** 319–333.

Grajkowski, W., Kubalski, A., and Koprowski, P. (2005). Surface changes of the mechanosensitive channel MscS upon its activation, inactivation, and closing. *Biophysics* **88,** 3050–3059.

Hall, J. E. (1975). Access resistance of a small circular pore. *J. Gen. Physiol.* **66,** 531–532.

Hamill, O. P., Marty, A., Neher, E., Sakmann, B., and Sigworth, F. J. (1981). Improved patch-clamp techniques for high-resolution current recording from cells and cell-free membrane patches. *Pflugers Arch.* **391,** 85–100.

Haswell, E. S., and Meyerowitz, E. M. (2006). MscS-like proteins control plastid size and shape in *Arabidopsis* thaliana. *Curr. Biol.* **16,** 1–11.

Hille, B. (1992). "Ionic Channels of Excitable Membranes." Sinauer Asssociates Inc., Sunderland, MA.

Hummer, G., Rasaiah, J. C., and Noworyta, J. P. (2001). Water conduction through the hydrophobic channel of a carbon nanotube. *Nature* **414,** 188–190.

Koch, A. L., and Woeste, S. (1992). Elasticity of the sacculus of *Escherichia coli*. *J. Bacteriol.* **174,** 4811–4819.

Koenig, B. W., and Gawrisch, K. (2005). Lipid-ethanol interaction studied by NMR on bicelles. *J. Phys. Chem. B* **109,** 7540–7547.

Koprowski, P., and Kubalski, A. (1998). Voltage-independent adaptation of mechanosensitive channels in *Escherichia coli* protoplasts. *J. Membr. Biol.* **164,** 253–262.

Koprowski, P., and Kubalski, A. (2003). C termini of the *Escherichia coli* mechanosensitive ion channel (MscS) move apart upon the channel opening. *J. Biol. Chem.* **278,** 11237–11245.

Levina, N., Totemeyer, S., Stokes, N. R., Louis, P., Jones, M. A., and Booth, I. R. (1999). Protection of *Escherichia coli* cells against extreme turgor by activation of MscS and MscL mechanosensitive channels: Identification of genes required for MscS activity. *EMBO J.* **18,** 1730–1737.

Li, Y., Moe, P. C., Chandrasekaran, S., Booth, I. R., and Blount, P. (2002). Ionic regulation of MscK, a mechanosensitive channel from *Escherichia coli*. *EMBO J.* **21,** 5323–5330.

Markin, V. S., and Martinac, B. (1991). Mechanosensitive ion channels as reporters of bilayer expansion. A theoretical model. *Biophysics* **60,** 1120–1127.

Martinac, B. (2001). Mechanosensitive channels in prokaryotes. *Cell Physiol. Biochem.* **11,** 61–76.

Martinac, B., Buechner, M., Delcour, A. H., Adler, J., and Kung, C. (1987). Pressure-sensitive ion channel in *Escherichia coli*. *Proc. Natl. Acad. Sci. USA* **84,** 2297–2301.

Martinac, B., Adler, J., and Kung, C. (1990). Mechanosensitive ion channels of, *E. coli* activated by amphipaths. *Nature* **348,** 261–263.

McLaggan, D., Naprstek, J., Buurman, E. T., and Epstein, W. (1994). Interdependence of K + and glutamate accumulation during osmotic adaptation of *Escherichia coli*. *J. Biol. Chem.* **269,** 1911–1917.

McLaggan, D., Jones, M. A., Gouesbet, G., Levina, N., Lindey, S., Epstein, W., and Booth, I. R. (2002). Analysis of the kefA2 mutation suggests that KefA is a cation-specific channel involved in osmotic adaptation in *Escherichia coli*. *Mol. Microbiol.* **43,** 521–536.

Miller, S., Bartlett, W., Chandrasekaran, S., Simpson, S., Edwards, M., and Booth, I. R. (2003a). Domain organization of the MscS mechanosensitive channel of *Escherichia coli*. *EMBO J.* **22,** 36–46.

Miller, S., Edwards, M. D., Ozdemir, C., and Booth, I. R. (2003b). The closed structure of the MscS mechanosensitive channel. Cross-linking of single cysteine mutants. *J. Biol. Chem.* **278,** 32246–32250.

Nomura, T., Yoshimura, K., and Sokabe, M. (2005). Exploring the lipid-protein interface essential to the mechanosensitivity of MscS, a mechanosensitive channel from, *E. coli*. *Biophys. J.* **88,** 290A.

Nomura, T., Yoshimura, K., and Sokabe, M. (2006). Voltage dependence of the adaptation in mscS occurs independent of the charged residues in the transmembrane domain. *Biophys. J.* **90,** XXA.

Okada, K., Moe, P. C., and Blount, P. (2002). Functional design of bacterial mechanosensitive channels. Comparisons and contrasts illuminated by random mutagenesis. *J. Biol. Chem.* **277,** 27682–27688.

Perozo, E., Kloda, A., Cortes, D. M., and Martinac, B. (2002). Physical principles underlying the transduction of bilayer deformation forces during mechanosensitive channel gating. *Nat. Struct. Biol.* **9,** 696–703.

Pivetti, C. D., Yen, M. R., Miller, S., Busch, W., Tseng, Y. H., Booth, I. R., and Saier, M. H., Jr. (2003). Two families of mechanosensitive channel proteins. *Microbiol. Mol. Biol. Rev.* **67,** 66–85, table.

Ruthe, H. J., and Adler, J. (1985). Fusion of bacterial spheroplasts by electric fields. *Biochim. Biophys. Acta* **819,** 105–113.

Sachs, F., and Morris, C. E. (1998). Mechanosensitive ion channels in nonspecialized cells. *Rev. Physiol. Biochem. Pharmacol.* **132,** 1–77.

Schleyer, M., Schmid, R., and Bakker, E. P. (1993). Transient, specific and extremely rapid release of osmolytes from growing cells of *Escherichia coli* K-12 exposed to hypoosmotic shock. *Arch. Microbiol.* **160,** 424–431.

Schumann, U., Edwards, M. D., Li, C., and Booth, I. R. (2004). The conserved carboxy-terminus of the MscS mechanosensitive channel is not essential but increases stability and activity. *FEBS Lett.* **572,** 233–237.

Shapovalov, G., and Lester, H. A. (2004). Gating transitions in bacterial ion channels measured at 3 micros resolution. *J. Gen. Physiol.* **124,** 151–161.

Sheetz, M. P., and Singer, S. J. (1974). Biological membranes as bilayer couples. A molecular mechanism of drug-erythrocyte interactions. *Proc. Natl. Acad. Sci. USA* **71,** 4457–4461.

Smart, O. S., Neduvelil, J. G., Wang, X., Wallace, B. A., and Sansom, M. S. (1996). HOLE: A program for the analysis of the pore dimensions of ion channel structural models. *J. Mol. Graph.* **14,** 354–360, 376.

Sotomayor, M., and Schulten, K. (2004). Molecular dynamics study of gating in the mechanosensitive channel of small conductance MscS. *Biophysics* **87,** 3050–3065.

Sotomayor, M., van der Straaten, T. A., Ravaioli, U., and Schulten, K. (2006). Electrostatic properties of the mechanosensitive channel of small conductance MscS. *Biophysics* **90,** 3496–3510.

Spelbrink, R. E., Kolkman, A., Slijper, M., Killian, J. A., and de, K. B. (2005). Detection and identification of stable oligomeric protein complexes in *Escherichi coli* inner membranes: A proteomics approach. *J. Biol. Chem.* **280,** 28742–28748.

Spronk, S. A., Elmore, D. E., and Dougherty, D. A. (2006). Voltage-dependent hydration and conduction properties of the hydrophobic pore of the mechanosensitive channel of small conductance. *Biophysics* **90,** 3555–3569.

Stewart, G. R., Patel, J., Robertson, B. D., Rae, A., and Young, D. B. (2005). Mycobacterial mutants with defective control of phagosomal acidification. *PLoS Pathog.* **1,** 269–278.

Strandberg, E., Ozdirekcan, S., Rijkers, D. T., van der Wel, P. C., Koeppe, R. E., Liskamp, R. M., and Killian, J. A. (2004). Tilt angles of transmembrane model peptides in oriented and non-oriented lipid bilayers as determined by 2H solid-state NMR. *Biophysics* **86,** 3709–3721.

Strop, P., Bass, R., and Rees, D. C. (2003). Prokaryotic mechanosensitive channels. *Adv. Protein Chem.* **63,** 177–209.

Sukharev, S. (2002). Purification of the small mechanosensitive channel of *Escherichia coli* (MscS): The subunit structure, conduction, and gating characteristics in liposomes. *Biophysics* **83,** 290–298.

Sukharev, S. I., Martinac, B., Arshavsky, V. Y., and Kung, C. (1993). Two types of mechanosensitive channels in the *Escherichia coli* cell envelope: Solubilization and functional reconstitution. *Biophysics* **65,** 177–183.

Sukharev, S. I., Blount, P., Martinac, B., Blattner, F. R., and Kung, C. (1994). A large-conductance mechanosensitive channel in, *E. coli* encoded by mscL alone. *Nature* **368,** 265–268.

Tieleman, D. P., Leontiadou, H., Mark, A. E., and Marrink, S. J. (2003). Simulation of pore formation in lipid bilayers by mechanical stress and electric fields. *J. Am. Chem. Soc.* **125,** 6382–6383.

Tsapis, A., and Kepes, A. (1977). Transient breakdown of the permeability barrier of the membrane of *Escherichia coli* upon hypoosmotic shock. *Biochim. Biophys. Acta* **469,** 1–12.

van der Straaten, T. A., Kathawala, G., Trellakis, A., Eisenberg, R. S., and Ravaioli, U. (2005). BioMOCA—a Boltzmann transport Monte Carlo model for ion channel simulation. *Mol. Simul.* **31,** 151–171.

Vasquez, V., and Perozo, E. (2004). Voltage dependent gating in MscS. *Biophys. J.* **86,** 545A.

Vora, T., Corry, B., and Chung, S. H. (2006). Brownian dynamics investigation into the conductance state of the MscS channel crystal structure. *Biochim. Biophys. Acta.* **1758,** 730–737.

Wesson, L., and Eisenberg, D. (1992). Atomic solvation parameters applied to molecular dynamics of proteins in solution. *Protein Sci.* **1,** 227–235.

Wood, J. M. (1999). Osmosensing by bacteria: Signals and membrane-based sensors. *Microbiol. Mol. Biol. Rev.* **63,** 230–262.

Wood, J. M., Bremer, E., Csonka, L. N., Kraemer, R., Poolman, B., van der, H. T., and Smith, L. T. (2001). Osmosensing and osmoregulatory compatible solute accumulation by bacteria. *Comp Biochem. Physiol. A Mol. Integr. Physiol.* **130,** 437–460.